DTIC FILE COPY

Naval Oceanographic and Atmospheric Research Laboratory Technical Note 39 June 1990



Preliminary Analysis of Low-Frequency Backscatter Data from the Blake Escarpment

AD-A226 492

plates: All DTIC reproduct...
tess will be in black and
white



M. M. Rowe
J. F. Gettrust
Seafloor Geosciences Division
Ocean Science Directorate

Approved for public release; distribution is unlimited. Naval Oceanographic and Atmospheric Research Laboratory, Stennis Space Center, Mississippi 39529-5004.

These working papers were prepared for the timely dissemination of information; this document does not represent the official position of NOARL.

ABSTRACT

Geoacoustic data acquired in the northern Blake-Bahama Basin by the Naval Oceanographic and Atmospheric Researth Laboratory's (NOARL's) Deep Towed Acoustics/Geophysics System (DTAGS) are used to estimate the distribution and strength of acoustic energy backscattered from the Blake Escarpment. The angular variability of backscatter sources on the Blake Escarpment is shown with scattering sections that present data steered at 0° (normal to the array) and -90° (endfire). The variability of the acoustic response of a promontory on the escarpment is shown on a shot-by-shot basis along the profile using frequency-wavenumber analysis. Migrated data (i.e., data where scattered energy has been transformed to the appropriate scattering surface) are used to estimate the size and distribution of scatterers; strong scatterers with lengths on the order of 100 m to over 1 km are identified. Low frequency (250 to scattering strengths of -27 dB/m2 are shown to be 650 Hz) appropriate for discrete scattering zones resolved with these data. preliminary analysis of pure-path geoacoustic demonstrates that such data can be used to obtain detailed information about the spatial distribution, size, and strength of seafloor scatterers.

Accession For

NTIS GRA&I
DTIC TAB
Unannonuced
Justification

By
Distribution/
Availability Codes

Availability Codes

Avail and/or
Dist
Special

50,000

ACKNOWLEDGMENTS

This work was funded by the Office of Naval Technology, Program Element 62435N, C. Votaw, program manager.

PRELIMINARY ANALYSIS OF LOW-FREQUENCY BACKSCATTER DATA FROM THE BLAKE ESCARPMENT

Introduction

Geoacoustic backscatter data collected along the Blake Escarpment (Site 3 in Figure 1) using the Naval Oceanographic and Laboratory's (NOARL's) Deep Research Acoustics/Geophysics System (DTAGS) provide the basis for a detailed study of the geoacoustic response of this major geologic feature. DTAGS is a deep towed multichannel system with a 205 dB // 1 μ Pa @ 1 m Helmholtz transducer source and two collinear arrays, each with 24 hydrophone groups (Figure 2). The array furthest from the source, the geophysical array, has hydrophone group offsets from 137 to 620 m with a group separation of 21 m; it is used to collect high resolution multichannel seismic data. near (acoustics) array has group offsets of 72 to 120 m with a group separation of 2.1 m. All hydrophone groups in these arrays are 1.8 m long and contain 6 omnidirectional hydrophones. A single calibrated hydrophone located 57 m from the source is used to obtain the source reference signature. The source signal used during this experiment is a 0.125 s linear FM sweep from 550 to 250 Hz (Figure 3).

The objective of this study was to obtain estimates of backscatter strengths of seafloor features and to spatially locate these sources of strong, coherent backscattered signals. The backscatter data were collected using the 24-channel acoustics array. This array can be steered from -90° to $+90^{\circ}$ relative to the track line. The beamwidths at 0° beam angle are 2.75° at 550 Hz and 6.0° at 250 Hz. At $+/-90^{\circ}$, the beamwidths are 12.5° at 550 Hz and 18° at 250 Hz. The system was towed at speeds ranging between 1.6 and 2.0 kn along a track that brought it within 400 m of the escarpment. Shots were fired every 30 seconds, resulting in a shot separation of 23 to 27 m. The data sample rate is 3125 samples/s/channel; the recording time window is 5.12 s.

Because of the omnidirectional source and the horizontal line array configuration, reflections from the left and right of the ship track cannot be separated. However, towing the system at mid water depth, just below the top of a large steep feature such as the Blake Escarpment, can mitigate left-right ambiguity within the data. The water depth at the base of the Blake Escarpment is 4950 m and the source and array were towed at a nominal depth of 2250 m above the seafloor; therefore, reflections from the sea surface arrive between 3.0 and 3.2 s. Although the Blake Escarpment is steep in geological terms (~35° slope), it extends far enough past the system to direct specular reflections from the bottom signals away from our array. Thus, it is not surprising that we can not identify a "bottom" reflection horizon in these data. The sea surface reflections (and, perhaps some seafloor returns) have been muted in the data presented in Figures 4 through 7. The water

surface/bottom reflection (Figures 4 and 5) is not flat because of vertical movement of the fish as it was towed along the track line.

The distance to scattering features is estimated using time of arrival with a water sound speed of 1511 m/s (as determined from a CTD cast); thus, with the $^{\circ}5.0$ s recording time window we can sample scatterers to a maximum range of 3780 m from the system.

Here we present the preliminary results from analysis of these backscatter data. Several different techniques have been used in this analysis to identify and characterize scattering sources on the Blake Escarpment. Work is in progress to refine the analysis techniques and absolute backscatter levels described below.

Data Processing - Beamforming

The data were band pass filtered from 250 to 550 Hz, and spectral balancing was applied to give a flat frequency response within that bandwidth. The data were then match filtered using the source signal recorded by the calibrated hydrophone. As the array shape is known from depth transducers mounted on the array 65 m and 126 m from the source, time shifts (< 0.03 s) were applied to correct the data to a horizontal datum prior to applying spatial filters to the data.

Although the data presented in Figures 4 and 5 look like standard multichannel seismic sections, here time is related to distance to the face of the escarpment rather than depth to a subbottom reflector. Figure 4 shows the range vs. time display of the data steered at 0° (broadside); this display shows the variability in reflectivity of the Blake Escarpment along the ship track (range) and downslope along the face of the escarpment (time). In Figure 4 strong backscattered energy centered at 2.4 km range with reflection times less than 1.0 s denote a promontory near the top of the escarpment that lies at a distance of 400 to 800 m from the trackline.

Figure 5 shows the data displayed as a function of range and time for the array steered at -90° (endfire, behind the array). Note the absence of the strong horizontal reflectors seen in Figure 4 between 2.5 to 3.5 s, the appearance of steeply dipping coherent reflections on the right hand side of the promontory, and the decreased amplitude of scattered energy from the promontory even when that feature is behind the array. The relative strengths of backscattered signals as a function of array steering direction give qualitative indications of the relative scattering area as a function of azimuth associated with those features. Thus, we infer that the promontory has a larger scattering area normal to the escarpment than it does (roughly) parallel to the escarpment. Similarly, low amplitude reflections to the right of the promontory (ranges from 3.25 to 5.0 km in Figure 4) have much higher amplitude when the array is steered to -90° (Figure 5).

Comparison of data with the array steered at 0° and -90° (Figures 4 and 5) suggests that the reflectors on the Blake Escarpment are characteristically narrow, linear features subparallel to the array. This linear, step-like reflection character also is observed in data for beam angles between 0° and +90°. Submarine photographs of the Blake Escarpment (Dillon et al., 1988) confirm the steplike nature of the face of the escarpment that we infer from our acoustic backscatter data.

Data Processing - Migration

The geoacoustic backscatter sections shown in Figures 4 and 5 include diffracted signals that are difficult to distinguish from specular reflections. Diffracted energy from corners of the promontory on the escarpment make that feature appear to be much wider than it actually is. To accurately identify the locations and dimensions of such features, the scattered energy must be migrated.

The migration process collects scattered energy in the data by summing amplitudes along the diffraction hyperbolae and locating the summed energy at the apex of each hyperbola. This process eliminates diffractions from the seismic section, enhances the acoustic image of the feature, and restores energy to the correct spatial position within the section.

To overcome spatial aliasing of the data, which is defined by the 23 m shot spacing, the instantaneous amplitude of the data was taken to obtain the envelope of the backscattered energy. These data were then low-pass filtered with a cutoff frequency of 60 Hz. The lower frequency envelope data together with the spatial filter inherent with stacking at 0° beam angle should eliminate all spatial aliasing. Figure 6 shows the unmigrated data, steered to 0° (shown in Figure 4), after taking the instantaneous amplitude and applying the low-pass filter.

Figure 7 shows the data in Figure 6 migrated at water sound speed (1511 m/s). Migration at water sound speed correctly places all energy scattered from the escarpment face that has not penetrated into the subbottom; any subbottom scattered energy will be attenuated. This gives us a first-order estimate of scattering levels from the escarpment. Examination of the data scattered from the highly lithified sediments that make up the escarpment (using a migration velocity of 2000 m/s) suggests that there is insignificant acoustic penetration of that feature.

Comparison of data presented in Figures 6 and 7 shows how the energy scattered from the rough escarpment face, appearing as high angle coherent reflections, has been restored to the sources of the scattering. The correct shape of the escarpment and the true lateral extent of the discontinuous horizontal reflecting horizons are shown in the migrated section in Figure 7. Note that the

promontory on the escarpment in the center of the section is significantly narrower than it appears to be in the unmigrated sections (Figures 4 and 6). With the unmigrated data, the promontory appears to extend from 0.0 to 4.2 km along the track. Migration of the data shows that it actually extends only from 1.0 to 3.5 km along the track. Further, the sides of the promontory are steeper than suggested by data shown in the unmigrated section (Figures 4 and 6) where the true position and slope of the side faces of the promontory are masked by diffraction hyperbolae from the corners of the promontory.

Coherent reflections arriving at later times in the section, such as those at 4.0 to 4.5 s between 2.0 and 3.0 km (Figures 6 and 7), also are restored to their correct position and size. Diffractions from the edges of these reflectors (Figures 4 and 6) appear to lengthen and shift them laterally within the section. Migration also has improved the signal-to-noise ratio of the backscattered signals, especially those arriving at later times (Figures 6 and 7). It is evident from the data presented in Figure 7 that the horizontal extent of significant scatterers range from 100 m to more than 1 km. As noted previously, the vertical extent of these scatterers is an order of magnitude less than their horizontal size.

Data Processing - F-K analysis

The promontory in the center of Figures 4 and 5 was tracked on a shot-by-shot basis in the f-k domain using a two-dimensional Fourier transform (converting time to frequency and range to wavenumber) using the 24 data traces associated with selected shots. The transform into wavenumber and frequency was used to determine the direction of arrival and frequency content of the backscatter from the escarpment. Figure 8 shows the relationship between wavenumber and grazing angle where grazing angle is the complement of beam angle. A 0.2 s window of the time series was chosen to isolate these reflections from the promontory.

Figure 9 shows 24 traces from a single shot (0.16 km range in Figure 4) used to compute the f-k display shown in Figure 10. The highest amplitude coherent reflections (Figure 9) are marked with a dashed line. At the time of this shot, the promontory was ahead of the array. A plot of the windowed, transformed data traces shows the strongly backscattered energy arriving from in front of the array at a grazing angle of 19°, or beam angle of 71°. Figures 10 through 12 track the reflection from the promontory as it approaches the array. In these figures energy arrives, respectively, at beam angles 71° (Figure 10), 28° (Figure 11), and 70° (Figure 12). F-k analysis of shots fired after the system passes by the promontory shows, as expected, that the maximum energy arrives from behind the array (at negative beam angles).

Figure 13 also shows the direction of arrival of the energy from the shot shown in Figure 9 but within a later time window, 2.2 to 2.4 s. (i.e., an arrival time greater than data presented in Figure 10). Comparison of the slope of the reflected signal across the traces within this time window with those arriving within the 1.5 to 1.7 s window demonstrates the ability of this system to discriminate between individual scatterers on the escarpment.

Note also in Figure 9, the time spread related to scattering from the escarpment. Interaction of the deconvolved source signal (*2.5 milliseconds in duration) with the escarpment results in significant backscattered signals extending for at least 3.0 s. The length of the time spread can be related to the geometry of the experiment in which the system was close to a long scattering surface, thus extending the relative difference in arrival times from scatterers along that feature.

Backscatter Levels

For these computations, the data were first corrected to account for spherical spreading. Then, relative backscatter signal levels were obtained by (1) taking the Fourier transform of the data and direct water path signals, then (2) computing the spectral ratio of the scattered to direct path data. This technique removes the system transfer function and yields amplitude ratios as a function of frequency relative to the (known) 205 dB // 1 μ Pa @ 1 m source. The inverse Fourier transform of this ratio represents the scattering levels over the frequency band sampled (250 to 650 Hz) as a function of time.

To obtain scattering strengths, the scattering levels must be corrected for the area insonified. The horizontal length sampled can be estimated from the known (6°) beamwidth. Because we are not working with simple geometries on the escarpment, we have chosen (after Hines, 1990) to estimate the vertical length by (1) measuring the time interval between -3 dB points for envelopes of the strong backscattered arrivals then, (2) multiplying half that two-way travel time by the compressional velocity in water.

Therefore, the estimates of scattering strength (in dB) are computed using the following formulation:

$$SS = Sr - So + 2R - A$$

where SS is the normalized scattering strength, Sr is the reflected signal level, So is the source level, R is the total transmission loss, and A is the bottom area insonified.

The data presented in Figure 14 are similar to those presented in Figure 4 but show scattering strength as a function of time and position. Note in Figure 14 that the strong, discrete backscatter zones have scattering strengths of approximately $-27~\mathrm{dB/m^2}$. Given

the relatively small areas associated with strong backscatter and geologic complexity of the region sampled, it is not possible to determine grazing angles associated with these scattering zones. However, our ability to resolve discrete scattering regions and estimate their low frequency scattering strengths provides a quantitative baseline for geoacoustic modeling of realistic marine environments.

Conclusions

This preliminary analysis of the backscattered data obtained using DTAGS shows that:

- o The direction of arrival of the peak received energy can be determined by steering the data along beam angles from -90° to +90°.
- o Sources of scattered energy along specific beams can be accurately located in space (range and time) by migrating the scattered energy using water sound speed.
- o Scattered energy from specific sources can be tracked as the instrument is towed by windowing the time series and performing a two-dimensional transform to the wavenumber and frequency domains.
- o Low frequency (250 to 650 Hz) backscatter strengths -27 dB/m² are associated with discrete scatterers with lengths on the order of 100 m to over 1 km on the Blake Escarpment.

Pure path backscattered geoacoustic data (i.e., data that have not interacted with the sea surface and have relatively short travel paths) can be used to obtain estimates of both the location and scattering strengths of geologic features at least as small as 100 m in extent. Development of similar data bases in geologic "type" regions will make possible predictions of both true geoacoustic scattering strengths and the spatial variability of scattering zones.

REFERENCES

- Dillon, W. P., A. W. Trehu, P. C. Valentine, and M. M. Bally, (1988). Eroded Carbonate Platform Margin the Blake Escarpment off Southeastern United States, in A. W. Bally, ed., Atlas of Seismic Stratigraphy, v. 2, Amer. Assoc. Petroleum Geologists Studies on Geology No. 27, 140-147 pp.
- Hines, P. C., (1990). Theoretical Model of Acoustic Backscatter from a Smooth Seabed. <u>JASA</u>, 88:324-334.

FIGURE CAPTIONS

- Figure 1: Location of DTAGS survey areas in the Blake-Bahama Basin. The data discussed in this technical note are from Site 3.
- Figure 2: Schematic of the DTAGS system showing the source and two (collinear) subarrays. Note that the system design places both low frequency (250 to 650 Hz) source and multichannel arrays at any desired depth (up to 6000 m). This flexibility makes it possible to conduct detailed studies anywhere within the ocean column.
- Figure 3: The DTAGS source signal and frequency spectrum are shown. The FM linear sweep signal is match filtered with the data to produce a Klauder wavelet of approximately 0.025 s duration.
- Figure 4: DTAGS backscatter data from the 0° (broadside) beam angle plotted as a function of range and time. The time window between 3.25 and 3.75 s has been muted to remove the sea surface reflection.
- Figure 5: DTAGS backscatter data from the -90° (endfire) beam angle plotted as a function of range and time. The time window between 3.25 and 3.75 s has been muted to remove the sea surface reflection.
- Figure 6: Instantaneous amplitude display of the backscatter data shown in Figure 4. The data were Hilbert transformed to obtain the envelope of backscattered signals then low-pass filtered at 60 Hz. The backscatter section presented here retains the essential character of that presented in Figure 4.
- Figure 7: DTAGS backscatter data in Figure 6 migrated at 1511 m/s. The envelope of the backscatter data (Figure 6) is used for migration to overcome spatial aliasing problems resulting from the ~23 m shot spacing.
- Figure 8: Diagram of wavefronts arriving at the array from a point scatterer ahead of the array and behind the array showing the relationship between beam angle, grazing angle, and wavenumber. K is wavenumber, w is angular frequency, λ is the wavelength of the arriving wavefronts, λ' is the design wavelength of the array, and ϕ is the grazing angle measured from parallel to the array. Beam angle, measured from perpendicular to the array, is the complement of the grazing angle.
- Figure 9: Data traces from the 24 independent hydrophone groups for a single shot, (shot 8 at 0.16 km range in Figures

- 4 and 5) are shown. Superimposed on the data are dashed lines identifying 5 coherent reflections that correspond to backscatter at different grazing angles (beam angles).
- Figure 10: Two-dimensional transform of the data presented in Figure 9 that lie between 1.5 and 1.7 s is displayed as a function of wavenumber and frequency. Peak energy has a wavenumber of 0.44 km⁻¹, corresponding to a grazing angle of nearly 19° to the array (in front of the array).
- Figure 11: Two-dimensional transform of data from a shot at 1.8 km range in Figures 4 and 5. The array is nearer to the promontory than in Figure 10. Peak energy is at 0.22 km⁻¹, corresponding to a grazing angle of 62° from parallel to the array.
- Figure 12: Two-dimensional transform of the shot at 2.8 km in Figures 4 and 5. Peak energy has wavenumber near 0, highest energy is arriving from directly perpendicular to the array, corresponding to a 90° grazing angle.
- Figure 13: Two-dimensional transform of the shot presented in Figure 9 with a time window between 2.2 and 2.4 s. (data from an earlier time window for the same shot are presented in Figure 10). Peak energy within this time window is arriving from perpendicular to the array (0°) and at -0.18 km⁻¹, -67°.
- Figure 14: Backscatter strength from the Blake Escarpment as a function of range and time. Peak backscatter strength (denoted by yellow regions) indicates reflection strengths greater than or equal to ~-30 dB/m². Note that the dark feature in the section that is observed between 3.5 and 3.75 s is related to the (muted) water surface reflection.

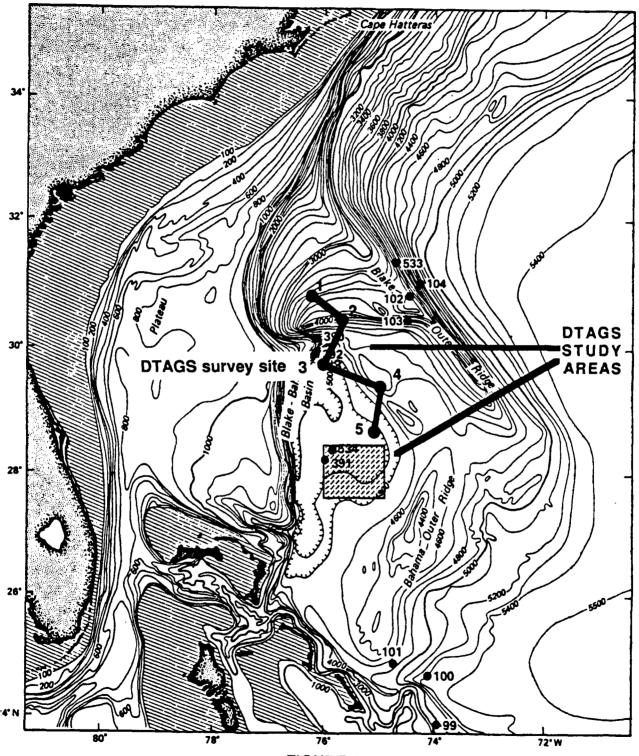
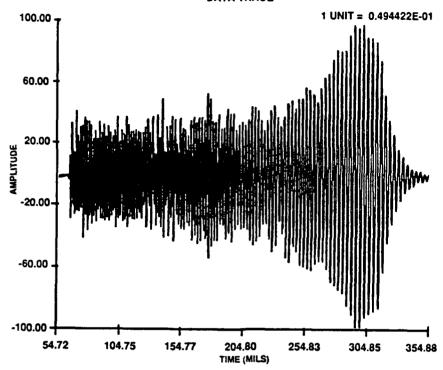


FIGURE 1

FIGURE 2

SPECTRUM ANALYSIS SHOT 1 SEQ. NO. 3 DATA TRACE



AMPLITUDE SPECTRUM

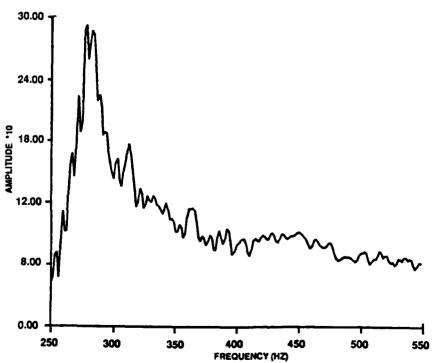
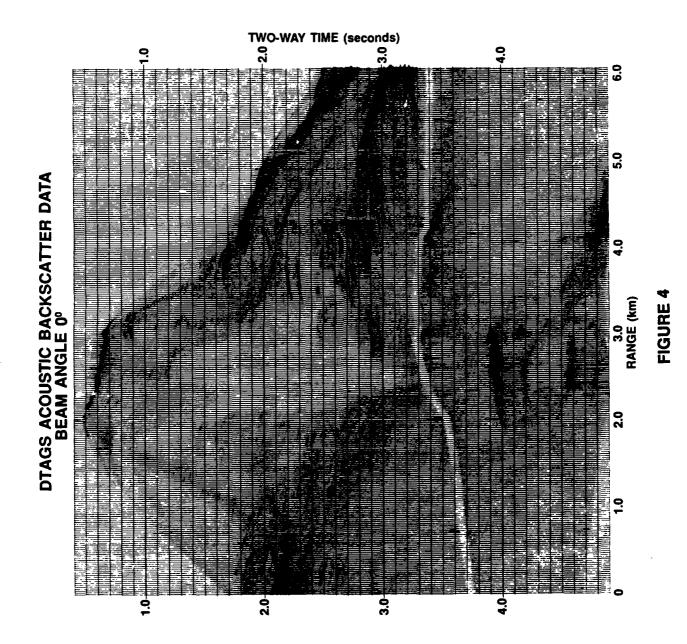
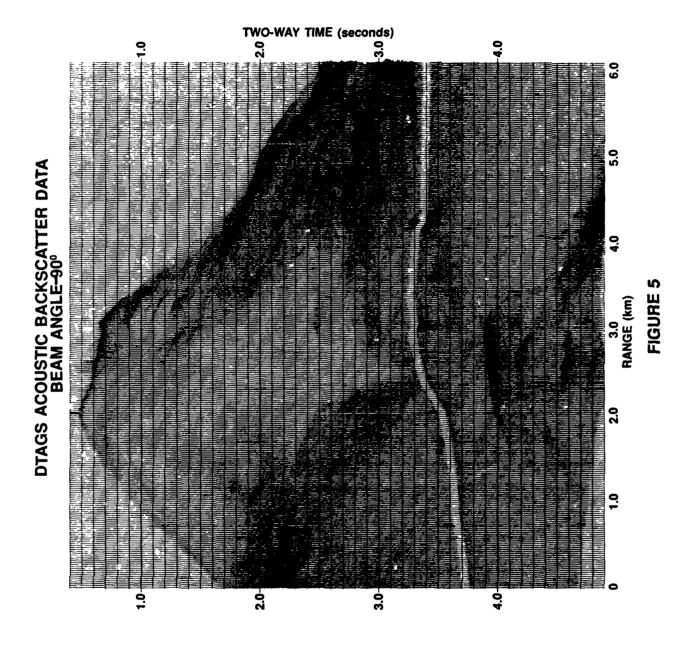
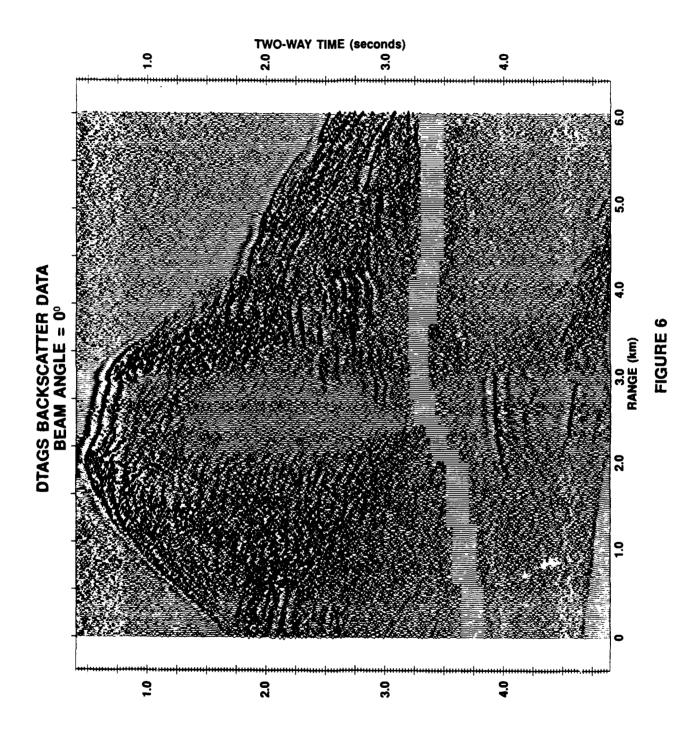
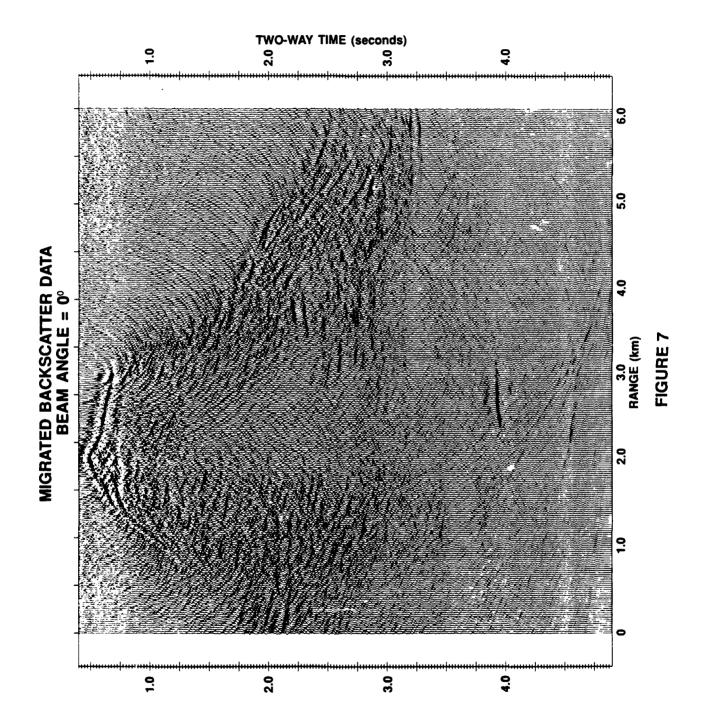


FIGURE 3

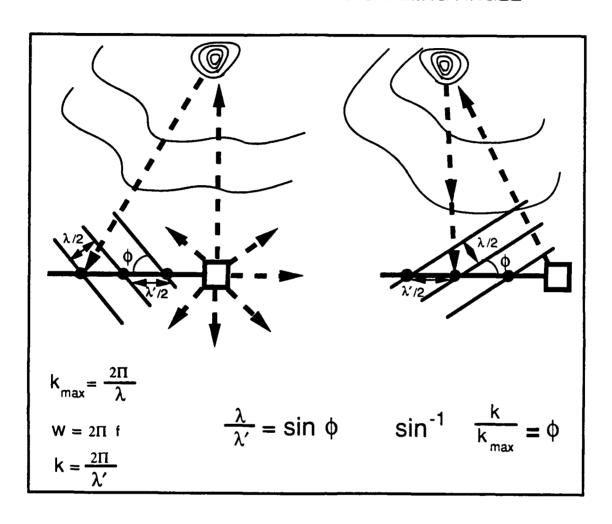








WAVE NUMBER RELATED TO GRAZING ANGLE



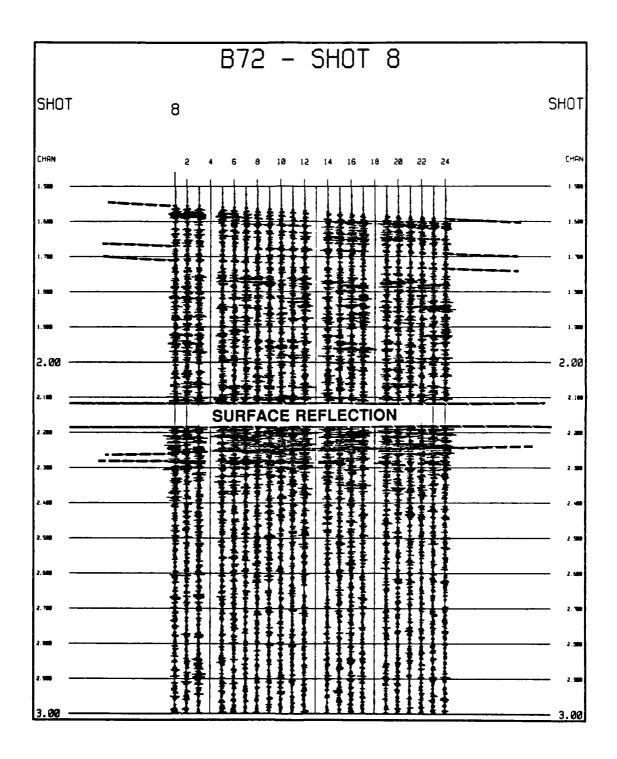
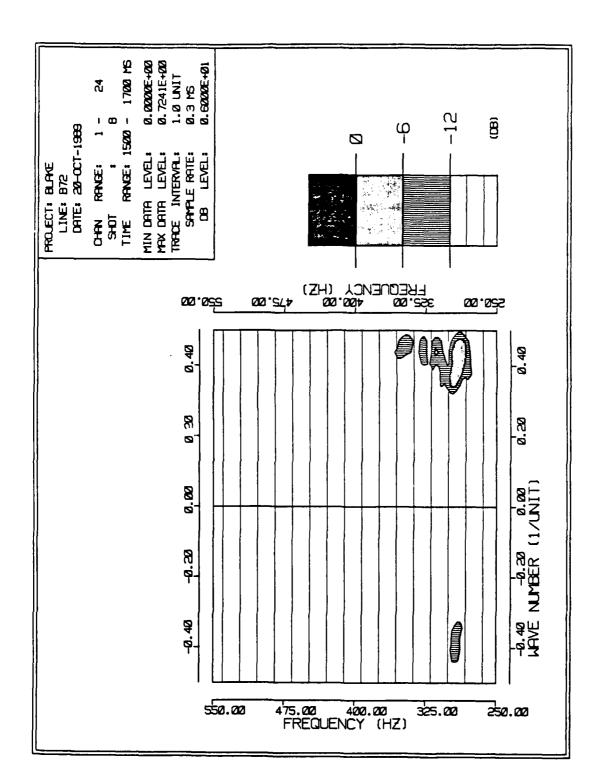


FIGURE 9



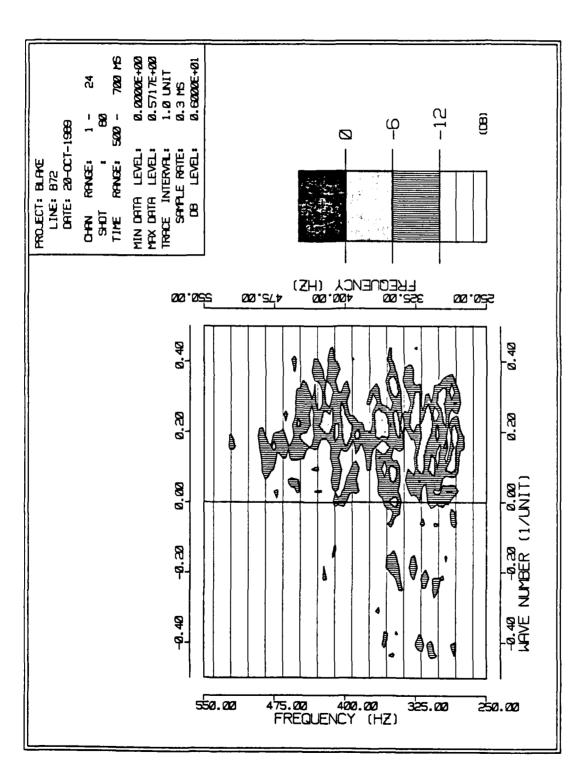
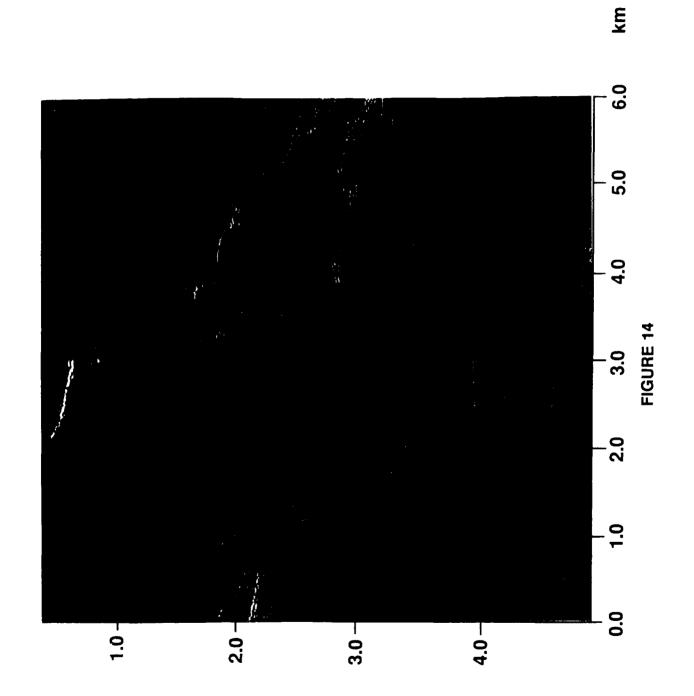


FIGURE 12

FIGURE 13

2 - WAY TIME (sec)



Distribution List

Naval Oceanographic and Atmospheric Research Laboratory Stennis Space Center, MS 39529-5004

Code 113
Code 125L (10)
Code 125P
Code 200
Code 244 (R. Slater)
Code 300
Code 360
Code 361 (M. Richardson, D. Lavoie, K. Fischer)
Code 362 (D. Bibee, S. O'Hara, J. Becklehimer, D. Lindwall)

NOARL Liaison Office (Brooke Farquhar) Crystal Plaza #5, Room 802 2211 Jefferson Davis Hwy Arlington, VA 22202-5000

Office of Naval Technology (C. Votaw, T. Goldsberry) 800 N. Quincy St. Arlington, VA 22217-5000

Office of Naval Research (M. Orr, J. Kravitz, R. Jacobson) 800 N. Quincy St. Arlington, VA 22217-5000

ONR Det. (E. Chaika) Stennis Space Center, MS 39529-5004

Naval Research Laboratory (D. Bradley) Washington, DC 20375

Officer in Charge Naval Underwater Systems Center Detachment New London Laboratory (M. Sundvick) New London, CT 06320

REPORT DOCUMENTATION PAGE

Form Approved OBM No. 0704-0188

Public reporting burden for this collection of information is estimated to average 1 hour per response, including the time for reviewing instructions, searching existing data sources, gathering and maintaining the data needed, and completing and reviewing the collection of information. Send comments regarding this burden or any other aspect of this collection of information, including suggestions for reducing this burden, to Washington Headquarters Services, Directorate for information Operations and Reports, 1215 Jefferson Davis Highway, Suite 1204, Arlington, VA 22202-4302, and to the Office of Management and Budget, Paperwork Reduction Project (0704-0188), Washington, DC 20503.

| 1. Agency Use Only (Leave blank). | 2. Report Date. June 1990 | 3. Report Type and Dates Covered. Interim | *** | |
|--|--|--|--|--|
| 4. Title and Subtitle. Preliminary Analysis of Low-F Data from the Blake Escarpm 6. Author(s). M. M. Rowe and J. F. Gettrus | S. Funding Numb Program Element Na. Project Na. Teak No Accession Na. | 62435N 030501 B02 DN258023 | | |
| 7. Performing Organization Names(Naval Oceanographic and Atr Ocean Science Directorate Stennis Space Center, Mississ | oratory Report Number | Report Number. NOARL Technical Note 39 | | |
| Sponsoring/Monitoring Agency Nat Office of Naval Technology 800 N. Quincy Street Arlington, VA 22217-5000 | Report Numb | 10. Sponsoring/Monitoring Agency Report Number. NOARL Technical Note 39 | | |
| 11. Supplementary Notes. | | | | |
| 12a. Distribution/Availability Statements Approved for public release; of | 12b. Distribution C | code. | | |
| Research Laboratory's (NOA distribution and strength of a backscatter sources on the Blato the array) and -90° (endfire on a shot-by-shot basis alon scattered energy has been to distribution of scatterers; stror (250 to 650 Hz) scattering of -6 | RL's) Deep Towed Acoustic energy backscalake Escarpment is shown. The variability of the ading the profile using frequency from the appropriate of the appropriate o | Bahama Basin by the Naval Oceanograph stics/Geophysics System (DTAGS) are untered from the Blake Escarpment. The anywith scattering sections that present data secustic response of a promontory on the equency-wavenumber analysis. Migrated data opriate scattering surface) are used to estimate or the order of 100 m to over 1 km are ident to appropriate for discrete scattering zones stic data demonstrates that such data care | sed to estimate the ingular variability of steered at 0° (normal scarpment is shown ita (i.e., data where timate the size and iffed. Low frequency resolved with these | |

| 14. Subject Terms. | 15. Number of Pages. 25 16. Price Code. | | | |
|---|---|--------------|--|---|
| (U) Directional Ambient Noise, (U) Bottom Scattering, (U) DTAGS, (U) OBS's (U) Towed Array | | | | |
| | | | 17. Security Classification of Report. | 18. Security Classification of This Page. |
| Unclassified | Unclassified | Unclassified | SAR | |